

Numerical calculation and analysis of hydrodynamic performance of a cylindrical oscillating float wave energy absorption device

Di Wang, Ke Xia, Decheng Wan *

Collaborative Innovation Center for Advanced Ship and Deep-Sea Exploration, State Key Laboratory of Ocean Engineering, School of Naval Architecture, Ocean and Civil Engineering, Shanghai Jiao Tong University, Shanghai, China

*Corresponding author: dcwan@sjtu.edu.cn

ABSTRACT

The point-absorber wave energy device has attracted researchers' attention for its efficiency and stability. In order to study the response of point-absorber wave energy generation device in wave, the motion of cylindrical floating body in wave is simulated in this paper. The CFD solver naoe-FOAM-SJTU based on open source platform OpenFOAM is used to simulate the motion performance of cylindrical power generation device under the regular wave. The wave response of the cylindrical floating body is analyzed and compared with the test. The motion of the single floating body and two floating bodies in the wave is simulated respectively. The interaction of the two floating bodies, the movement characteristics of the body under different conditions are analyzed. The damping coefficient is introduced to reflect the influence of generator on the motion of cylindrical floating body in wave. Through the calculation of theoretical wave energy conversion efficiency, the factors affecting the conversion efficiency of wave energy are discussed.

Key words: wave power converter; naoe-FOAM-SJTU solver; wave load; energy conversion efficiency

1 INTRODUCTION

In the background of the increasing consumption of fossil fuels, the new type of renewable energy as an alternative source of energy is more and more concerned by governments and researchers. As a representative non-polluting renewable energy, the research of wave energy collection device has been carried out for many years. Today, although there have been many models of wave power devices, the overall development of the wave power generation device is still relatively low. There are many factors contributing to this situation, among which the characteristics of wave and wave energy collection devices are the main constraints. Wave energy is widely distributed in nature, but with low density and unstable characteristics, there is no condition for large-scale mining. At the same time, wave energy collection devices generally have higher requirements for mooring system, which make the cost of single wave power generation system higher. In addition, the stability of wave energy collection device has become the bottleneck of large-scale application of wave energy. Although many ingenious devices have high collection efficiency, its reliability is poor, which make it easy to be damaged under the conditions of the extreme sea conditions. These factors makes the exploitation of wave energy still far behind the use of wind energy.

Although many wave energy absorption devices have been developed, especially the famous Salter duck wave absorption device¹ of which peak absorption efficiency of wave energy has reached an astonishing 80 %, the complex structure and high manufacturing cost limit its large-scale promotion. At present, many

researchers are inclined to simple point absorption device, especially cylindrical device².

The separated cylindrical floating body is generally used as a floating breakwater for marine engineering³. The cylinder is placed on the surface and perpendicular to the direction of the wave. When the wave reaches the floating body, part of the energy is reflected, and part of the energy is converted into the kinetic energy of the cylindrical floating body. Some of the kinetic energy will be emitted by the cylinder, and the remaining energy will be stored as electricity or consumed because of the damping effect.

There has been a lot of research on the wave energy absorption device. Ringwood and Butler⁴ find that for a wave energy absorption device, when the damping coefficient is relatively small, the conversion efficiency of the wave energy decreases with the increase of the wave frequency, when the damping coefficient is large, the opposite is true. Nolan et al.⁵ used numerical method to analyze the optimal damping coefficient for wave energy conversion efficiency. Pastor and Liu⁶ used experimental and numerical simulation methods to analyze the wave energy absorption device, found that the larger the float diameter, the more wave energy absorption. Through Bing Chen⁷'s experiments and numerical calculation, the characteristics of single and two floating body wave absorption devices are calculated and analyzed. In this paper, the characteristics of the two floating bodies' wave absorption devices will be further studied on the basic of Bing Chen.

A clever design can balance the efficiency and production cost, so that the cylindrical power plant can play the maximum effect. To make the design more reasonable, it is necessary to study the response of the cylindrical floating body waves under varies wave conditions.

A viscous flow solver naoe-FOAM-SJTU which is developed and based on the popular open source toolbox OpenFOAM is presented to simulate the response of cylindrical floating body in wave, and the calculated results are compared with the experimental results. Then, the motion and force of the single floating body and two floating bodies with different damping coefficients are compared and analyzed, and the characteristics of the floating body damping movement in the wave are found. Finally, the wave energy conversion efficiency of the cylindrical floating body is calculated, and the variation characteristics of the efficiency of single floating body and two floating bodies are analyzed. It provides a reference for the design of point-absorber wave energy device.

2 NUMERICAL METHOD

2.1 Governing equation

The general control equations of incompressible and viscous fluids are:

$$\nabla \cdot \mathbf{U} = 0 \quad (1)$$

$$\frac{\partial \rho \mathbf{U}}{\partial t} + \nabla \cdot (\rho (\mathbf{U} - \mathbf{U}_g) \mathbf{U}) = -\nabla p_d - \mathbf{g} \cdot \mathbf{x} \nabla \rho + \nabla \cdot (\mu \nabla \mathbf{U}) \quad (2)$$

In which, \mathbf{U} is fluid velocity, \mathbf{U}_g is velocity of mesh grid, p_d is dynamic pressure of fluid, the value is equal to difference between the total pressure and the hydrostatic pressure. \mathbf{g} is acceleration of gravity, ρ is density of fluid, μ is dynamic viscosity coefficient.

$k-\omega$ SST turbulence model is used in this paper, and wall function is used in the near wall surface. The finite volume method (FVM) is used to discrete the equation, and the PISO algorithm is used to solve the velocity pressure coupling problem. The free surface is captured by the fluid volume method (VOF).

2.2 Motion of floating cylinders

In this paper, the cylindrical floating body only has motion in the vertical direction, the equation is:

$$m\ddot{z} + C\dot{z} = G + F_w \quad (3)$$

In which, m is mass of the cylinder, \dot{z} and \ddot{z} are heave speed and acceleration respectively. C is damping coefficient, G is volume force of cylinder, F_w includes wave force and hydrostatic buoyancy. $C\dot{z}$ consists of generator load, transmission resistance and generation loss. In this paper, the value of damping coefficient C is changed to study the motion response and stress of cylindrical floating body under different damping coefficients.

2.3 Wave generation theory

The wave generated in this paper is modelled on a wave module called waves2foam8 developed by OpenFOAM. According to the wave parameters used in the experiment, it can be found that all wave conditions belong to the range of stokes second order wave, so this paper uses stokes second order wave theory to make wave, and its approximate solution is:

$$\phi = \varepsilon\phi_1 + \varepsilon^2\phi_2 \quad (4)$$

In which ε is perturbation parameter, ϕ_1 and ϕ_2 are first order and second order solution.

Waves2foam produces waves by changing the speed inlet boundary conditions. The control equation of the relaxation region is:

$$\alpha_R(\chi_R) = 1 - \frac{\exp(\chi_R^{3.5}) - 1}{\exp(1) - 1} \text{ for } \chi_R \in [0,1] \quad (5)$$

In which, α_R is relaxation factor, which is a function of χ_R . Its trends are as follows:

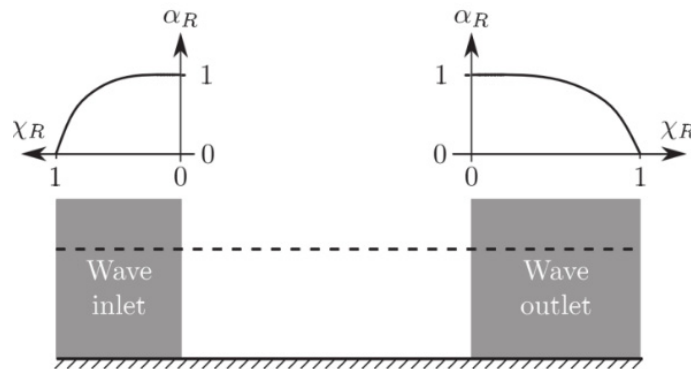


Fig. 1 α_R trend in inlet and outlet region

The effect of relaxation factor is:

$$\phi = \alpha_R\phi_{computed} + (1 - \alpha_R)\phi_{target} \quad (6)$$

In which ϕ is velocity of free surface or liquid parameter.

From Fig 1, the wave strength will increase from 0 and remain stable at the entrance. The maximum value will be reduced to 0 at the exit. The relaxation area at the inlet and outlet will form the wave area and

the wave area of the numerical pool.

3 NUMERICAL MODEL AND TEST CONDITIONS

3.1 Physical model and numerical model

The numerical model of the cylindrical floating device is shown in fig. 2, the test device is as shown in fig. 3, the test tank is 60 meters long, 4 meters wide, and 2.4 meters deep. On one side of the pool there is a piston wave generator, on the other side is the wave beach. The cylindrical float model is made of organic glass, 1 meter long and 0.2 m in diameter. The cylinder is fixed by the iron rod and ensures that it has degrees of freedom only in the vertical direction. The experiment was completed at the national key laboratory of coastal and offshore engineering of Dalian university of technology.⁷

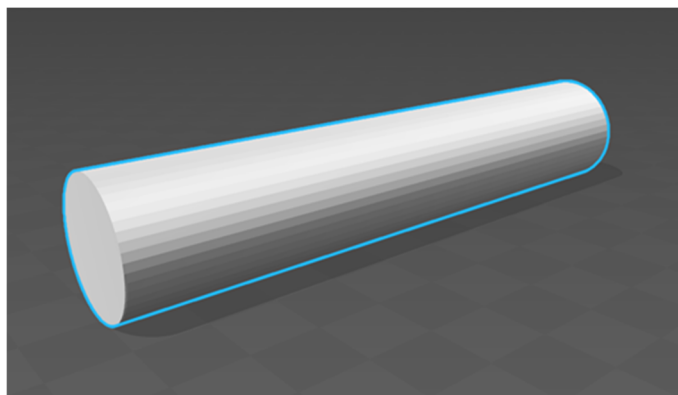


Fig.2 Single cylinder model



Fig.3 Experiment device

3.2 Mesh and computational domain

In this paper, snappyHexMesh9, a mesh solver of OpenFOAM is used to extract mesh grid of body surface. The total mesh number is around 1.5 million.

Figure 4 shows the total computational domain size used in this paper. The computational domain grid guarantees a length of one wave length before the float, and two or three wave lengths after the float, to ensure the full evolution of the waves. Figure 5 and Figure 6, respectively, show the single-cylinder and double-cylinder floating body and its nearby grid distribution.

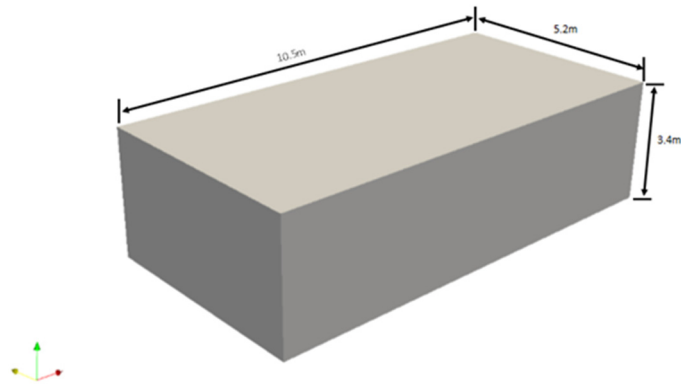


Fig.4 Computational domain

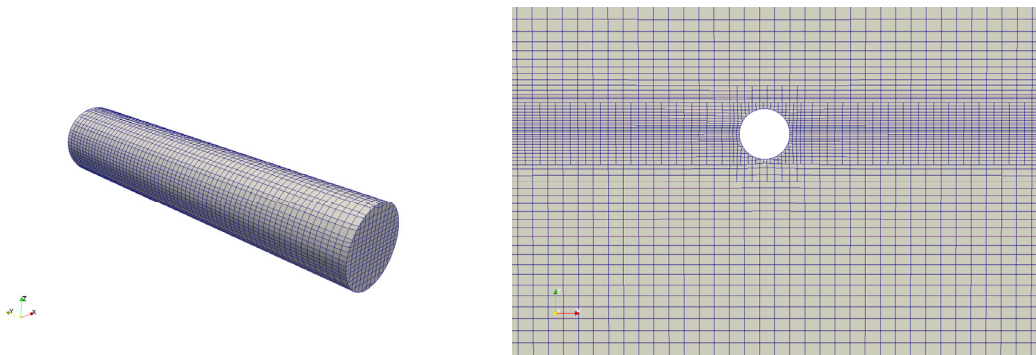


Fig.5 Grid distribution of single cylinder

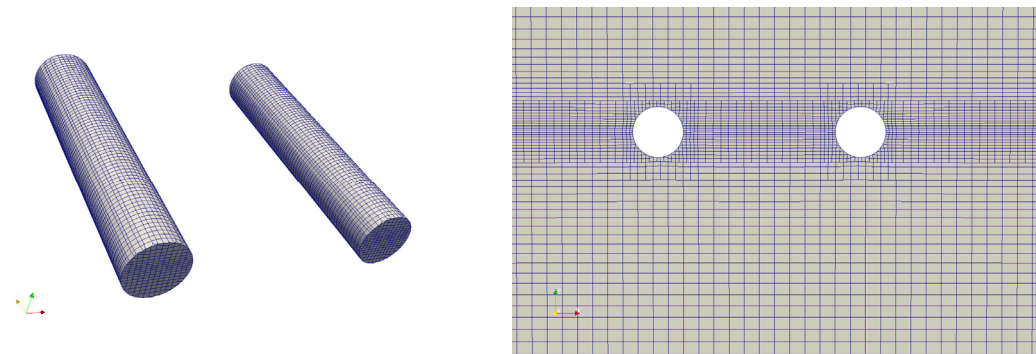


Fig.6 Grid distribution of double cylinder

3.3 Calculating conditions

The main calculation conditions are shown in the following table, in which the experimental condition is no2, which is to verify the accuracy of the numerical calculation method. In addition, the results of several other numerical examples will be compared with the results of Chen et al.7 , and the influence of different calculation methods on the results will be analyzed.

Table.1 Parameter for numerical simulation

Case no.	Wave height H (m)	Period T (s)	Wave length L (m)	Number of cylinder	Diameter D (m)	Mass m (kg)
1	0.1	1.5	3.35	1	0.1	3.93
2					0.2	15.70
3					0.3	35.33
4		1.3	2.60	2	0.2	15.70
5		1.5	3.35			
6		1.7	4.11			

4 RESULT AND ANALYSIS

4.1 Validation of numerical model.

In this paper, the results of 3D numerical simulation are compared with the experimental and two-dimensional CFD results made by Chen et al. The comparison with the test can verify the accuracy of CFD calculation, and provide support for the subsequent calculation and analysis. The time - calendar curve for calculating and comparing the results is shown in figure 7. As shown in the figure, the results of 3D calculation using naoeFOAM are in good agreement with the experiment, and the results are more accurate than the two - dimensional CFD calculation. This proves the accuracy of 3D CFD results. At the same time, the results of 3D calculation show that there is a slight waveform inconsistency with the test: the peak value have a certain stagger. This is mainly because this paper uses waves2foam to create stokes second order wave to make it consistent with the actual situation, but the experiment uses linear wave, which results in a subtle difference in waveform. In general, the three-dimensional calculation results are in good agreement with the experimental results, which can ensure the accuracy of further calculation. Fig.8 is a flow field image when the wave is stable.

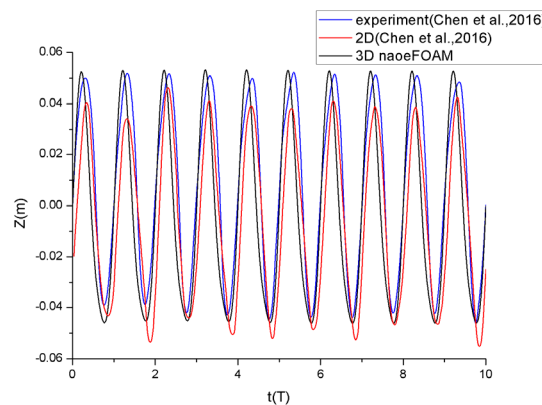


Fig 7. Time series of measured and predicted heave displacement of single cylinder

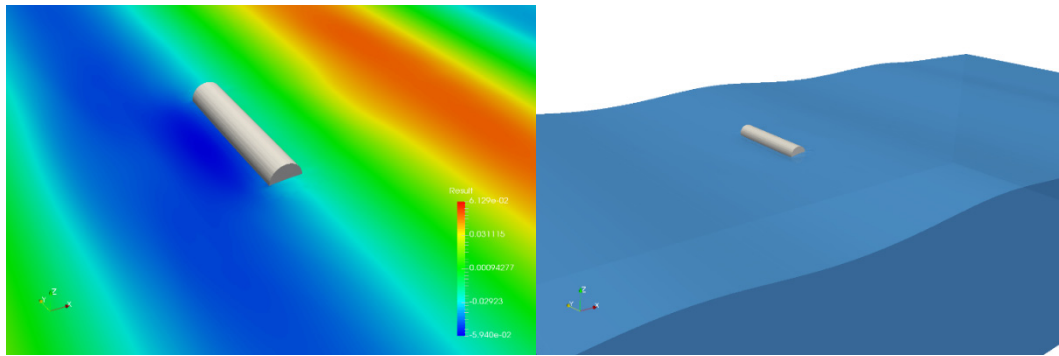


Fig 8. Flow field of single cylinder

Compared with the 3D CFD results, the results of Chen's two-dimensional calculation show the deviation of the amplitude and the instability of the wave. Fig. 9 shows the vertical displacement of one cylinder in the case of a wave height of 0.1 m, a wave period of 1.5s, and the damping coefficient is $C=400\text{N}/(\text{m}/\text{s})$. The curve shows the two-dimensional results are slightly lower than the three - dimensional results, but the overall similarity is relatively high. The reason for this deviation may be that the two-dimensional calculation does not consider the influence of the length of the floating body, the wave will bypass both sides of the floating body, which will affect movement of cylinder.

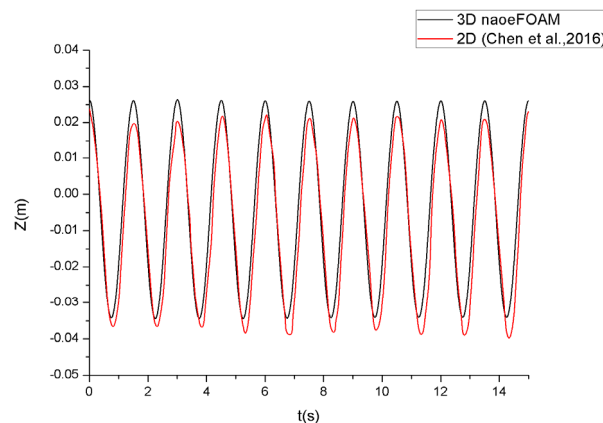
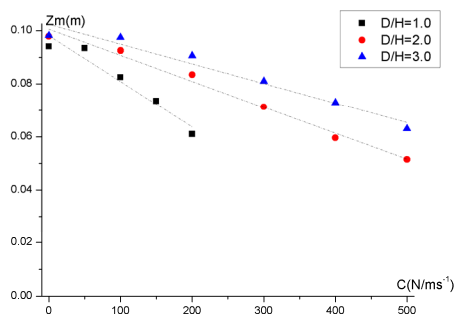


Fig.9 Time series of measured and predicted heave displacement of single cylinder with $C=400\text{N}/(\text{m}/\text{s})$

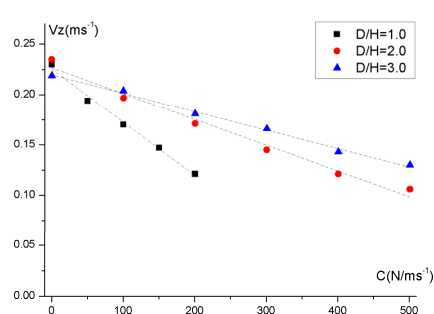
4.2 Cylinders' heave motion

The motion of the floating body is very important for the design of energy output device, and the understanding of the displacement and velocity of the floating body affects the design and selection of the hydraulic system.

Fig.10 shows the heave motion of a single cylinder under different damping coefficients. In which C is the damping coefficient, Z_m is the displacement amplitude, which size is equal to the maximum displacement minus the minimum displacement. The V_z is the maximum speed of the heave motion. As shown from fig. 10, the displacement amplitude and velocity of heave motion decreases linearly with the increase of damping coefficient. The change rate of displacement and velocity decreases with the increase of the diameter of the cylinder.



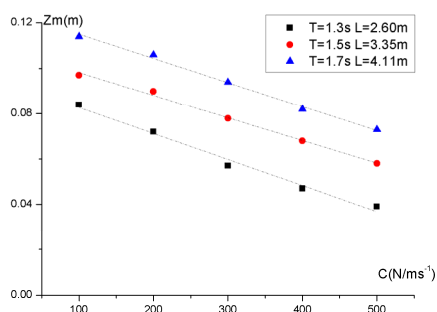
(a) Magnitude of displacement



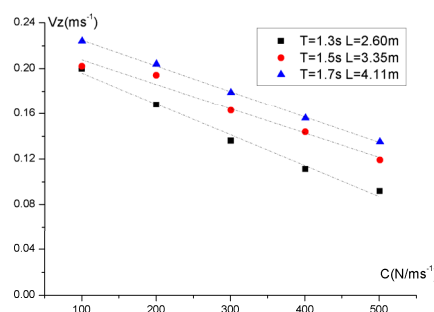
(b) Maximum of heave speed

Fig.10 Heave motion of single cylinder

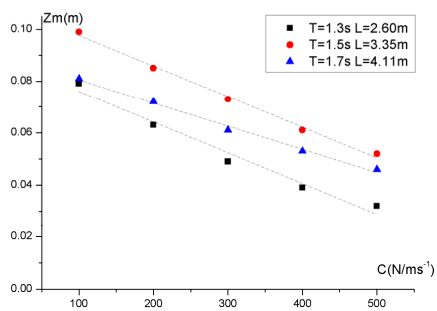
Fig.11 shows the heave motion of a double cylinder under different damping coefficients. The displacement amplitude and maximum velocity of the double cylinder decreases linearly with the increase of the damping coefficient. Through Fig.11 (a)(b), for the first cylinder, the displacement amplitude and maximum velocity increase with the increase of period and wavelength. The three fitting lines in Fig.11(a) are almost parallel, indicating that the change in damping coefficient is almost equal to the effect of the first cylinder in different wavelength and period conditions. Figure 11(c)(d) well reflects the interaction between the two cylinders. Under the action of the first cylinder, the second cylinder is not only different from the first cylinder in the value of the displacement amplitude and the maximum vertical velocity, but also distinct in the change rate for different wave length.



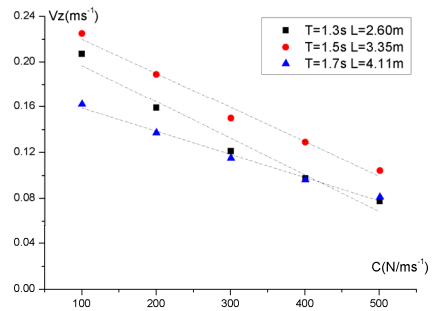
(a) Displacement magnitude of 1st cylinder



(b) Maximum heave speed of 1st cylinder



(c) Displacement magnitude of 2nd cylinder



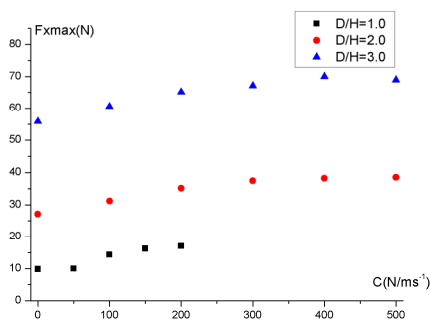
(d) Maximum heave speed of 2nd cylinder

Fig.11 Heave motion of double cylinders

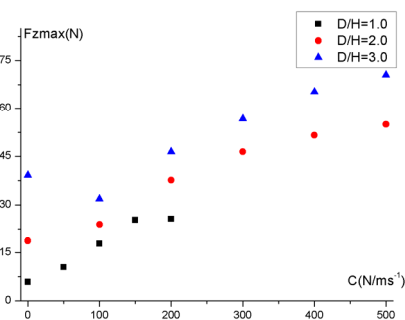
4.3 Wave load on cylinder

Wave load is very important for the design of wave energy collection device. Fig.12 shows the wave force of a single cylinder. The F_{xmax} and F_{zmax} are the maximum wave forces in the horizontal and numerical direction, respectively

Both horizontal wave force and vertical wave force increase with the increase of the diameter of the cylinder. Both horizontal wave force and vertical wave force increase with the increase of damping coefficient. The amplitude of horizontal wave force increases with the damping coefficient is smaller than the vertical wave force. When the damping coefficient is large, the increase of horizontal wave force is nearly 0, and increase of vertical wave force become smooth.



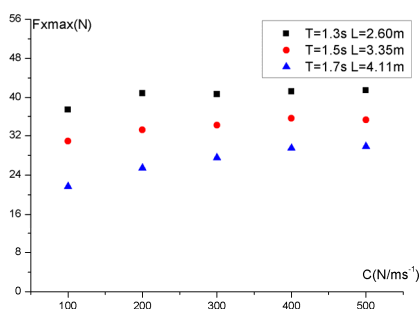
(a)Horizontal wave force



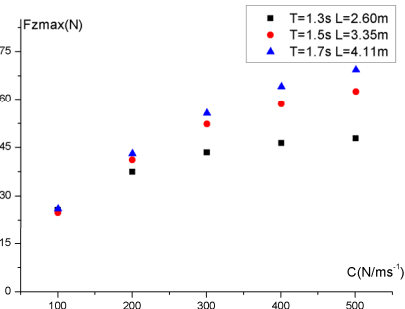
(b)Vertical wave force

Fig.12 Wave force on single cylinder

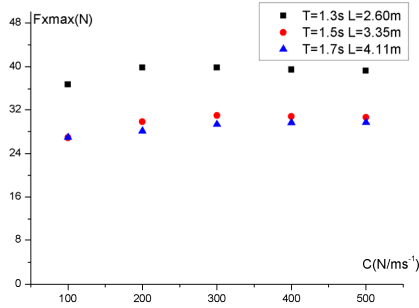
Fig.13 shows the wave load of double cylinder. Fig.13(a)(b) shows the longer the wavelength, the larger horizontal wave forces on the first cylinder, and the vertical wave forces are the opposite. The wave force of the first cylinder increases with the increase of damping, and the horizontal wave force increases relatively slowly. When the damping coefficient is small, the vertical wave force at different wavelength is almost equal, and the vertical wave force between different wavelength is obviously different with the increase of damping coefficient. Fig.13(c)(d) show the wave force trend of the second cylinder is approximate to the first cylinder, but at $T=1.5s$, $L=3.35m$ and $t=1.7s$, $L=4.11m$ the horizontal wave force difference is small. The vertical wave force variation trend of the second cylinder is obviously different from the first cylinder, which reflects the interference between the two cylinders.



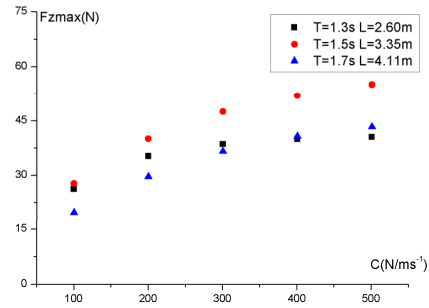
(a)Horizontal force on 1st cylinder



(b)Vertical force on 1st cylinder



(c) Horizontal force on 2nd cylinder



(d) Vertical force on 2nd cylinder

Fig.13 Wave force on double cylinder

4.4 Wave energy conversion efficiency

Wave energy conversion efficiency is the key parameter for the wave energy collection device. Wave energy can be understood as a cylinder converts part of its kinetic energy into electrical energy by the motor damping work, the primary conversion formula is:

$$P_0(t) = |F_{damp} \cdot \dot{z}| = |C\dot{z} \cdot \dot{z}| \quad (7)$$

In which \dot{z} is vertical speed of cylinder, C is damping coefficient, the wave energy converted from t_1 to t_2 can be expressed as:

$$\bar{P}_0 = \int_{t_1}^{t_2} P_0(t) dt / (t_2 - t_1) \quad (8)$$

According to the results of Toyota et al.10, the wave energy of unit width is obtained by the following formula:

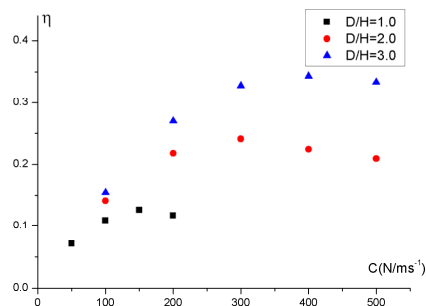
$$P_{wave} = \frac{\pi}{2kT} \rho g \left(\frac{H}{2}\right)^2 \left(1 + \frac{2kh}{\sinh 2kh}\right) \quad (9)$$

Primary wave energy conversion efficiency is:

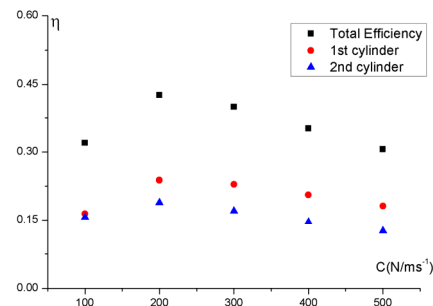
$$\eta = \frac{\bar{P}_0}{P_{wave}} \quad (10)$$

Fig. 14 shows the wave energy conversion efficiency of a single and double cylinder under different conditions. Fig.14(a) shows that the larger the cylinder diameter, the higher the wave energy conversion efficiency. The peak of wave energy conversion efficiency of different diameters is also different, the larger the diameter, the larger the damping coefficient corresponding to the peak wave energy conversion efficiency. Fig.14(b)(c)(d) show the difference in wave energy conversion efficiency under different wave conditions. The first cylindrical wave energy conversion efficiency is always higher than the second cylinder, the gap between the two will increase with the increase of damping coefficient. When T=1.7s, L=4.41, the first cylinder wave energy conversion efficiency is significantly higher than the second, and this phenomenon is not observed

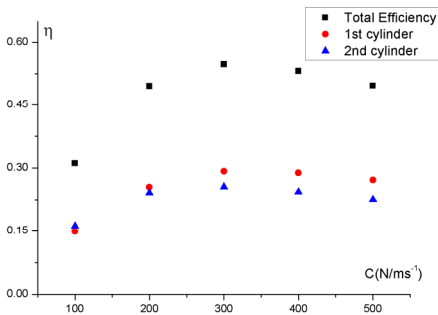
under the other two wavelengths. Fig.14 (e) shows the total conversion efficiency of wave energy under different wave conditions. It can be found that the peak value of wave energy conversion efficiency is different under different wave conditions, and the location of the peak is different. This means that for the same wave energy converter device, there is a wave condition that can reach the most efficiency. It is necessary to understand the effect of wave conditions on efficiency to design a more efficient device.



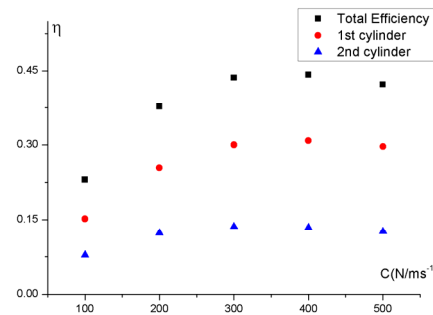
(a) Single cylinder



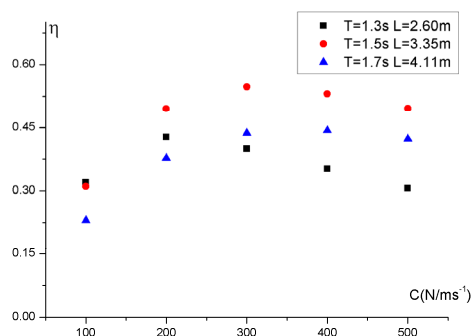
(b) Double cylinder when T=1.3s, L=2.60m



(c) Double cylinder when T=1.5s, L=3.35m



(d) Double cylinder when T=1.7s, L=4.41m



(e) Total efficiency of double cylinder

Fig.14 Primary wave energy conversion efficiency versus damping coefficients

5 CONCLUSIONS

In this paper, the naoe-FOAM-SJTU solver based on OpenFOAM is used to simulate the wave response and the energy conversion efficiency of a single cylindrical floating body and two cylindrical floating bodies. In this paper, firstly, the response of single floating body in wave is analyzed, and the comparison of time

domain curves with the experiments and references is carried out. Through comparison, the calculated results are in good agreement with the test results, which provides a basis for further calculation. Then, the numerical simulation of a single cylinder with different damping coefficient and diameter is carried out. From the calculation results, the displacement and velocity of a single floating body is strongly linear with damping coefficient, and is affected by diameter of cylinder. Through the study of the force of the floating body, it can be found that the force of the cylindrical floating body increases with the increase of damping coefficient, and the double floating body has the mutual influence on the horizontal force and vertical force. Finally, the wave energy conversion efficiency under different damping coefficients is calculated, and the characteristics of single floating body and multiple floating wave energy conversion efficiency are compared. It is found that there is an ideal damping coefficient that makes wave energy conversion efficiency reach the highest. In this paper, the characteristics of the wave energy absorption device of the cylindrical floating body are calculated and analyzed, and provide some reference for the future design of wave energy device.

ACKNOWLEDGEMENTS

This work is supported by the National Natural Science Foundation of China (51379125, 51490675, 11432009, 51579145), Chang Jiang Scholars Program (T2014099), Shanghai Excellent Academic Leaders Program (17XD1402300), Shanghai Key Laboratory of Marine Engineering (K2015-11), Program for Professor of Special Appointment (Eastern Scholar) at Shanghai Institutions of Higher Learning (2013022), Innovative Special Project of Numerical Tank of Ministry of Industry and Information Technology of China(2016-23/09) and Lloyd's Register Foundation for doctoral student, to which the authors are most grateful.

REFERENCES

1. Salter, S.H., 1974. Wave power. *Nature* 249 (5459), 720–724.
2. Kofoed, J.P., 2009. Hydraulic Evaluation of the DEXA Wave Energy converter. Aalborg University.
3. Ozeren, Y., Wren, D.G., Altinakar, M., Work, P.A., 2011. Experimental investigation of cylindrical floating breakwater performance with various mooring configurations. *J. Waterw. Port. Coast. Ocean. Eng.* 137 (6), 300–309.
4. Ringwood, J., Butler, S., 2004. Optimisation of a wave energy converter. *CAMS* 2004, 155–160.
5. Nolan, G.A., Ringwood, J.V., Leithead, W., Butler, S., 2005. Optimal damping profiles for a heaving buoy wave-energy converter. In: *Proceedings of the International Offshore and Polar Engineering Conference Proceedings*, vol. 1, pp. 477–485. ISSN 1098-6189.
6. Pastor, J., Liu, Y., 2014. Power absorption modeling and optimization of a point absorbing wave energy converter using numerical method. *J. Energy Resour. Technol.* 136 (2), 021207.
7. Chen B, Ning D, Liu C, et al. Wave energy extraction by horizontal floating cylinders perpendicular to wave propagation[J]. *Ocean Engineering*, 2016, 121:112-122.
8. OpenFOAM. Mesh generation with the snappyHexMesh utility. 2013. Available from: <http://www.openfoam.org/docs/user/snappyHexMesh.php#x26-1510005.4>.
9. Niels G.Jm David R.F, Jorgen F., A wave generation toolbox for the open-source CFD library: OpenFOAM®. Available from: <https://www.researchgate.net/publication>
10. Toyata, K., Nagata, S., Imai, Y., Setoguchi, T., 2013. Experiments and numerical analysis on conversion efficiency of floating pendulum wave energy converter in regular waves. *Proceedings of the 23rd International Offshore Polar Engineering* vol. 1, 552–559.